Powder XRD and TEM study on crystal structure and interstratification of Zn-chlorite (baileychlore)

Seungyeol Lee, and Huifang Xu[a)]
Department of Geoscience, NASA Astrobiology Institute, University of Wisconsin – Madison, Madison, 53706 Wisconsin

(Received 9 March 2017; accepted 26 March 2017)

Baileychlore is Zn-end member trioctahedral chlorite, named by Audrey C. Rule and Frank Radke in 1988 for the honor of Professor Sturges W. Bailey of the University of Wisconsin – Madison, USA. Baileychlore occurs as dark green chlorite on calcite veins from garnet-vesuvianite skarn clasts at Red Dome ore deposit, Chillagoe, Queensland, Australia. The baileychlore has been studied by using powder X-ray diffraction (XRD), transmission electron microscopy (TEM), and X-ray energy-dispersive analytical electron microscopy analyses to determine crystal structure and interstratified layers. Baileychlore with stacking disorder displays streaking reflections of $0k0$ ($\neq 6n$) hhl ($h \neq 3n$). Unit-cell parameters for baileychlore (type I polytype) with a space group of $C\bar{1}$ are: $a = 5.351(3)$, $b = 9.266(5)$, $c = 14.418(8)$ Å, $\alpha = 89.741(3)°$, $\beta = 96.741(4)°$, and $\gamma = 90.122(2)°$. The strong lines of the measured XRD pattern [d(Å)(I)(hkl)] are: 14.331(7.151)(90.5)(002); 4.574(23.2)($1\bar{1}0$, $11\bar{1}$); 3.572(38.5)(004); 2.653(31.4)($\bar{1}31$, 200, $13\bar{1}$); 2.406(49.4)(202, $\bar{1}33$, $13\bar{3}$); 1.543(27.6)($\bar{3}31$, 060, $33\bar{1}$), respectively. Reitveld refinement provides a composition $(Zn_{2.49}Al_{0.09}Fe^{2+}_{0.09}\square_{0.33})^{0.61-}$ for the octahedral sheet and $(Si_{3.53}Al_{0.47})^{0.47-}$ for the tetrahedral sheets within the 2:1 layer with $(Al_{1.08}Fe_{1.08}Mg_{0.84})^{1.08+}$ for the interlayer sheet. The refinement results indicate that baileychlore is an intergrowth of type I and II polytypes. High-resolution TEM images show stacking disorder of baileychlore with small amount of isolated smectite layers. © *2017 International Centre for Diffraction Data*. [doi:10.1017/S0885715617000410]

Key words: baileychlore, XRD, Reitveld refinement, TEM, polytypes, interstratification

I. INTRODUCTION

Chlorite is a common mineral in hydrothermal ore deposits, metamorphic rocks, and retrograde reaction products of igneous rocks (Veblen and Ferry, 1983; Bowman *et al.*, 1987; Chernosky *et al.*, 1988; Laird, 1988; Xu *et al.*, 1990; Xu and Veblen, 1993; Jacquat *et al.*, 2008). Mg and Fe are common elements in trioctahedral chlorite in addition to Si, Al, H, and O (Dunn *et al.*, 1987; Bailey, 1988). However, the elements Mn, Ni, Co, Zn, and Cu are considered as trace elements in chlorite, because they commonly occur in chlorite with very low concentration (Bailey, 1988; Veblen, 1992). Unusually, high-concentrated Zn-bearing chlorite (ZnO 28–30 wt%), baileychlore was reported from drill hole at Red Dome mine, located near Chillagoe, Australia (Rule and Radke, 1988). The Zn-chlorite occurs as replacements of altered andesite and skarn clasts (Smith, 1985; Torrey *et al.*, 1986). In this paper, we used X-ray diffraction (XRD), transmission electron microscopy (TEM), and X-ray energy-dispersive spectroscopy (EDS) spectra to better understand the crystal structures and interstratification of baileychlore.

II. SAMPLE AND EXPERIMENTAL METHODS

We studied baileychlore samples from a drill hole at Red Dome deposit (Rule and Radke, 1988). The baileychlore in the specimen shows dark green color, which is associated with yellow or brown montmorillonite locally (Figure 1). We picked a dark green grain for powder XRD and TEM analysis. XRD data were collected on a two-dimensional (2D) image-plate detector using a Rigaku Rapid II instrument (Mo$K\alpha$ radiation) in the Geoscience Department. The 2D images were converted to produce conventional 2θ vs. intensity patterns using Rigaku's 2DP software. The detailed crystal structure of baileychlore was calculated using the Rietveld refinement method with TOPAS 5 software. A pseudo-Voigt function was used for fitting the peak profiles. TEM samples were prepared by coating distilled water suspensions of crushed baileychlore onto carbon-coated 200-mesh Cu grids. TEM images and selected-area electron diffraction (SAED) analyses were carried out using a Philips CM200-UT microscope operated at 200 kV in the Materials Science Center at the University of Wisconsin – Madison. The chemical composition was analyzed by TEM–EDS spectra using a Si:Li detector (Oxford instruments Link ISIS) with a beam diameter of ~50 nm (spot size 5).

III. RESULTS AND DISCUSSION

The powder XRD pattern of baileychlore indicates poor crystallinity, with broad $02l$ and $11l$ peaks (Figure 2). The shapes of the peaks (streaking toward high angle) at $d = 4.6$ and ~2.6 Å are suggestive of stacking disorder in adjacent layers (Figure 2). The broad peak at ~2.6 Å is related to the streaking of $20l$ and $13l$ reflections resulting from stacking

[a)]Author to whom correspondence should be addressed. Electronic mail: hfxu@geology.wisc.edu

https://doi.org/10.1017/S0885715617000410 Published online by Cambridge University Press

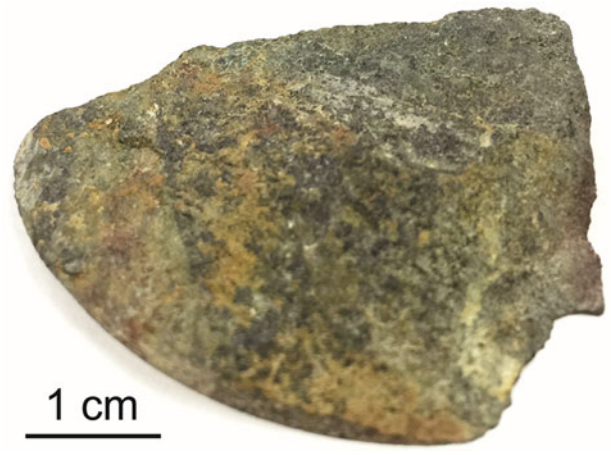


Figure 1. (Color online) Hand specimen of baileychlore. Dark green part is baileychlore; yellow and brownish parts are montmorillonite.

of TOT layers because of opposite octahedral orientations (Xu and Veblen, 1993). The *d*-values for the (001) and (002) peaks slightly increased after being ethylene glycolated (Figure 2), which confirms the presence of interstratified smectite layers. Chlorite is a 2:1:1 phyllosilicate that cannot be collapsed or expanded by normal laboratory procedures (Bailey and Brown, 1962; Bayliss, 1975). The 7.211 Å of the (002) peak of treated baileychlore indicates the presence of ~10% of randomly interstratified smectite mixed layers in chlorite layers (Reynolds, 1988; Shau *et al.*, 1990). Previous differential thermal and thermogravimetric analyses of baileychlore also support the smectite layers within baileychlore, indicated by a loss of water at 120–200 °C (Olives, 1985; Rule and Radke, 1988).

Rietveld refinement analyses were performed to calculate the structural parameters of baileychlore based on space group of $C\bar{1}$ with two polytype structures (Figures 3 and 4). For the refinement, we used the previously reported chemical formula

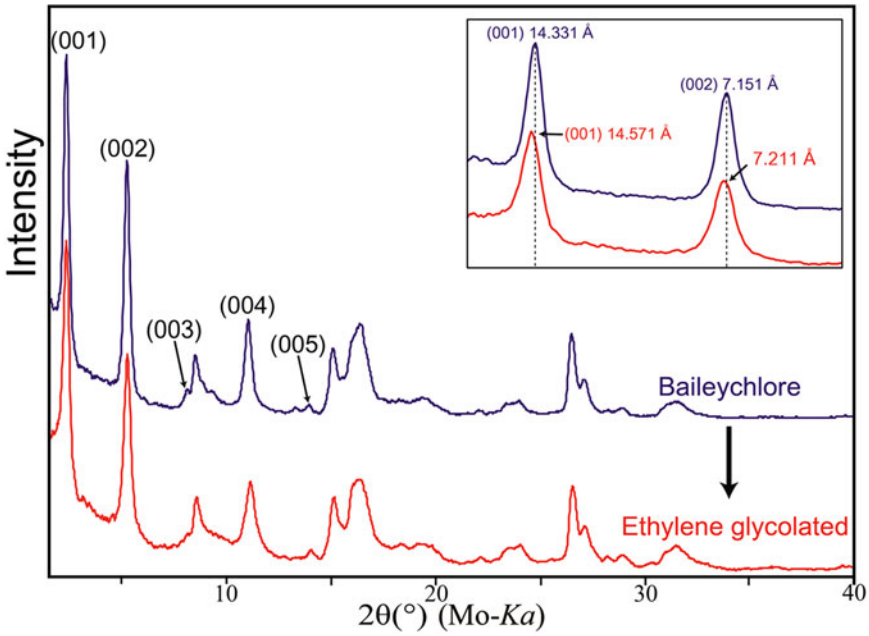


Figure 2. (Color online) XRD patterns of baileychlore (blue) and that of ethylene glycolated sample (red).

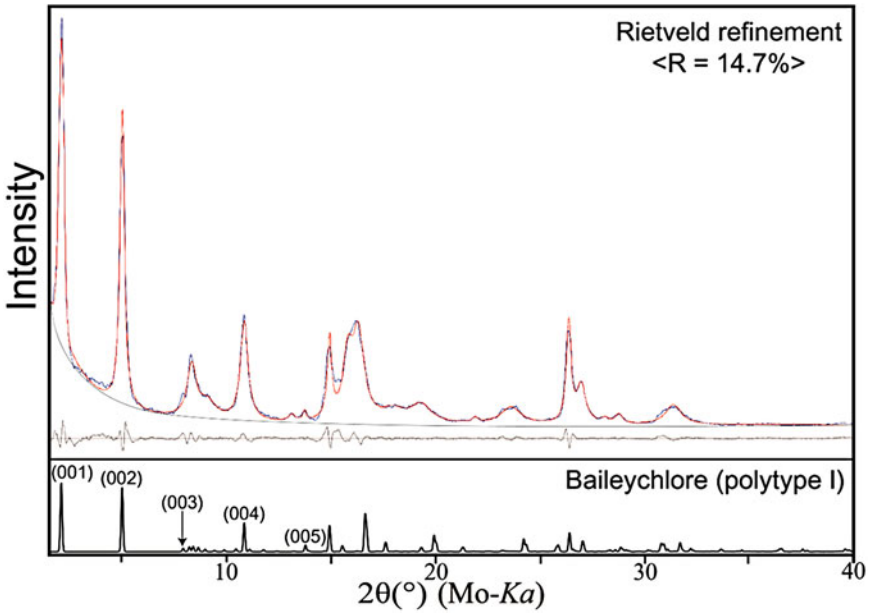


Figure 3. (Color online) Rietveld refinement of XRD pattern of baileychlore using type I polytype. The residual between measured and calculated patterns is illustrated at the upper-right corner of the XRD pattern.

https://doi.org/10.1017/S0885715617000410 Published online by Cambridge University Press

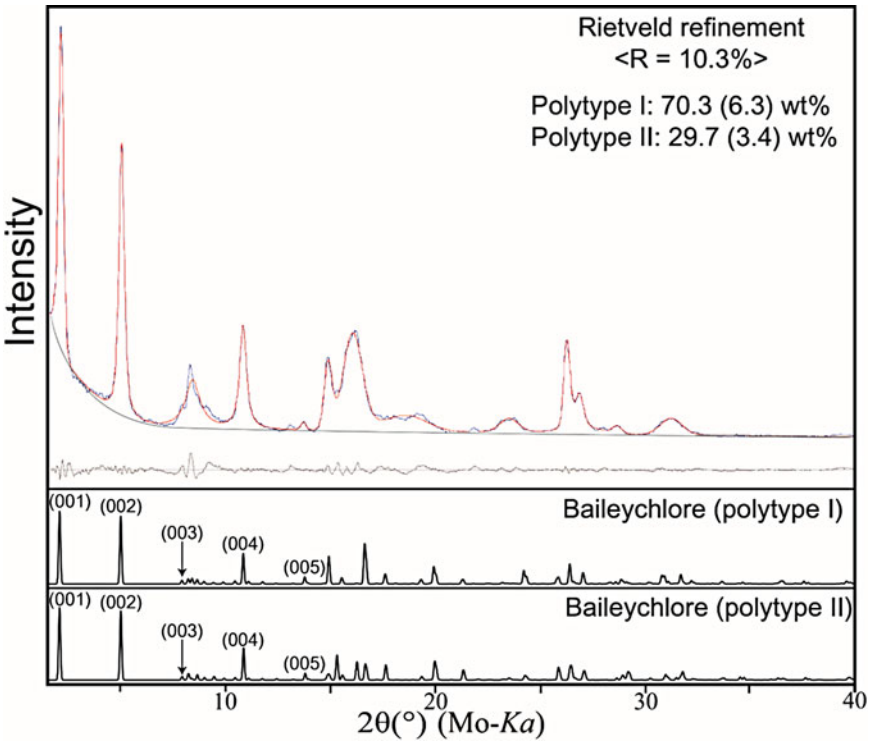


Figure 4. (Color online) Rietveld refinement of XRD pattern of baileychlore with intergrowths of type I and II domains. The residual between measured and calculated patterns is illustrated at the upper-right corner of the XRD pattern.

of baileychlore $(Zn_{2.50}Fe^{2+}_{1.20}Al_{1.17}Mg_{0.76}Mn^{2+}_{0.01}\square_{0.36})[Si_{3.55}\ Al_{0.45}]O_{10}(OH)_8$, analyzed by using electron microprobe (Rule and Radke, 1988). Fractional coordinates and occupancies for the structure of baileychlore polytypes I and II are listed in Tables I and II, respectively. We repeatedly refined each atom coordinates and checked the values from staring structures to avoid errors from highly correlated variables after unit-cell parameter refinement. Rule and Radke (1988) used I*b* symmetry for least-squares refinement; however, triclinic $C\bar{1}$ is the more reasonable symmetry because

TABLE I. Atomic coordinates of baileychlore: type I polytype.

Space group ($C\bar{1}$)

Atom	Occupancy	*x*	*Y*	*z*
ZnM1	0.83	0.000 (2)	0.000 (2)	0.000 (1)
AlM1	0.03	0.000 (2)	0.000 (2)	0.000 (1)
FeM1	0.03	0.000 (2)	0.000 (2)	0.000 (1)
ZnM2	0.83	0.999 (3)	0.333 (4)	0.002 (2)
AlM2	0.03	0.999 (3)	0.333 (4)	0.002 (2)
FeM2	0.03	0.999 (3)	0.333 (4)	0.002 (2)
AlM3	0.36	0.003 (5)	0.166 (3)	0.504 (2)
FeM3	0.36	0.003 (5)	0.166 (3)	0.504 (2)
MgM3	0.28	0.003 (5)	0.166 (3)	0.504 (2)
AlM4	0.36	0.000 (1)	0.500 (2)	0.500 (2)
FeM4	0.36	0.000 (1)	0.500 (2)	0.500 (2)
MgM4	0.28	0.000 (1)	0.500 (2)	0.500 (2)
Si1	0.88	0.400 (1)	0.001 (1)	0.191 (2)
Al1	0.12	0.400 (1)	0.001 (1)	0.191 (2)
Si2	0.88	0.894 (5)	0.167 (2)	0.428 (3)
Al2	0.12	0.894 (5)	0.167 (2)	0.428 (3)
O1	1.00	0.360 (2)	0.996 (3)	0.075 (3)
O2	1.00	0.860 (3)	0.171 (4)	0.076 (1)
O3	1.00	0.133 (2)	0.065 (2)	0.232 (3)
O4	1.00	0.645 (4)	0.100 (1)	0.232 (1)
O5	1.00	0.931 (5)	0.328 (3)	0.234 (3)
OH1	1.00	0.381 (3)	0.333 (1)	0.074 (2)
OH2	1.00	0.154 (3)	0.998 (3)	0.432 (1)
OH3	1.00	0.129 (3)	0.339 (2)	0.428 (1)
OH4	1.00	0.653 (4)	0.164 (2)	0.428 (3)

Lattice parameters: $a = 5.351$ (3), $b = 9.266$ (5), $c = 14.418$ (8), $\alpha = 89.741$ (3), $\beta = 96.861$ (4), $\gamma = 90.122$ (2)

TABLE II. Atomic coordinates of baileychlore: type II polytype.

Space group ($C1$)

Atom	Occupancy	*x*	*y*	*z*
ZnM1	0.83	0.000 (1)	0.000 (1)	0.000 (2)
AlM1	0.03	0.000 (1)	0.000 (1)	0.000 (2)
FeM1	0.03	0.000 (1)	0.000 (1)	0.000 (2)
ZnM2	0.83	0.002 (2)	0.334 (3)	0.000 (1)
AlM2	0.03	0.002 (2)	0.334 (3)	0.000 (1)
FeM2	0.03	0.002 (2)	0.334 (3)	0.000 (1)
AlM3	0.36	0.999 (4)	0.167 (3)	0.500 (5)
FeM3	0.36	0.999 (4)	0.167 (3)	0.500 (5)
MgM3	0.28	0.999 (4)	0.167 (3)	0.500 (5)
AlM4	0.36	0.000 (1)	0.500 (2)	0.500 (1)
FeM4	0.36	0.000 (1)	0.500 (2)	0.500 (1)
MgM4	0.28	0.000 (1)	0.500 (2)	0.500 (1)
Si1	0.88	0.233 (2)	0.169 (5)	0.192 (4)
Al1	0.12	0.233 (2)	0.169 (5)	0.192 (4)
Si2	0.88	0.733 (3)	0.002 (1)	0.192 (5)
Al2	0.12	0.733 (3)	0.002 (1)	0.192 (5)
O1	1.00	0.194 (2)	0.167 (1)	0.077 (3)
O2	1.00	0.694 (3)	0.001 (2)	0.077 (3)
O3	1.00	0.211 (1)	0.336 (3)	0.233 (1)
O4	1.00	0.515 (3)	0.105 (2)	0.233 (2)
O5	1.00	0.015 (2)	0.067 (3)	0.233 (2)
OH1	1.00	0.692 (3)	0.334 (4)	0.073 (4)
OH2	1.00	0.158 (1)	0.999 (4)	0.431 (2)
OH3	1.00	0.135 (4)	0.340 (2)	0.430 (1)
OH4	1.00	0.635 (4)	0.158 (3)	0.430 (3)

Lattice parameters: $a = 5.351$ (5), $b = 9.266$ (3), $c = 14.418$ (6), $\alpha = 90.122$ (3), $\beta = 96.861$ (4), $\gamma = 89.741$ (5)

https://doi.org/10.1017/S0885715617000410 Published online by Cambridge University Press

TABLE III. Powder X-ray data for baileychlore with type I and II polytypes.

I_{obs}	d_{obs}	d_{clac}(I)	I_{clac}(I)	d_{clac}(II)	I_{clac}(II)	*hkl*
1000	**14.331**	14.315	1000	14.315	1000	001
905	**7.151**	7.157	935	7.157	944	002
46	4.762	4.772	49	4.772	51	003
132	**4.574**	4.612	55	4.600	32	$1\bar{1}0$
		4.520	57	4.535	20	$11\bar{1}$
385	**3.572**	3.579	426	3.579	423	004
61	2.869	2.863	92	2.863	87	005
314	**2.653**	2.657	124	2.648	24	$\bar{1}31$
		2.656	138	2.656	24	200
		2.650	127	2.659	26	$13\bar{1}$
59	2.571	2.558	36	2.558	24	201
		2.557	27	2.558	24	$\bar{1}32$
494	**2.406**	2.399	228	2.399	92	202
		2.397	222	2.387	91	$\bar{1}33$
		2.387	221	2.397	84	$13\bar{3}$
73	2.273	2.275	49	2.275	73	133
		2.270	50	2.271	73	$1\bar{3}3$
		2.266	49	2.266	73	$20\bar{4}$
59	2.083	2.084	24	2.082	16	134
		2.078	22	2.080	17	$1\bar{3}4$
134	2.021	2.021	106	2.021	109	204
		2.019	105	2.010	108	$\bar{1}35$
		2.009	105	2.018	113	$13\bar{5}$
37	1.896	1.899	24	1.897	50	135
		1.894	24	1.896	48	$1\bar{3}5$
		1.891	21	1.891	48	$20\bar{6}$
124	1.675	1.678	79	1.678	27	206
		1.676	81	1.670	27	$\bar{1}37$
		1.669	80	1.675	26	$13\bar{7}$
276	**1.543**	1.546	80	1.542	82	$\bar{3}31$
		1.544	82	1.544	83	060
		1.543	81	1.548	83	$33\bar{1}$
107	1.508	1.510	24	1.514	25	331
		1.508	25	1.510	28	$06\bar{2}$
		1.506	27	1.512	28	$33\bar{3}$
51	1.435	1.431	24	1.431	23	0010
32	1.415	1.418	14	1.419	13	$\bar{3}35$
		1.333	47	1.332	7	139
92	1.331	1.330	46	1.332	7	$1\bar{3}9$
		1.328	46	1.328	7	$20\bar{1}0$

of the semi-random stacking. The calculated unit cell parameters of baileychlore are: $a = 5.351(3)$, $b = 9.266(5)$, $c = 14.418(8)$ Å, $\alpha = 89.741(3)°$, $\beta = 96.741(4)°$, and $\gamma = 90.122(2)°$. The calculated density of baileychlore is 3.183 g cm^{-3}, which is analogous to the measured density 3.18(2) g cm^{-3}. The final fitting result of two polytype structures (Figure 4) indicates the presence of domains of type I and II chlorite, which can be considered as an approximation for the partially disordered chlorite. The type II polytype is the stable structure in high-temperature metamorphic rocks (Walker, 1993).

Reitveld refinement provides a composition of $(Zn_{2.49}Al_{0.09}Fe^{2+}_{0.09}\square_{0.33})^{0.61-}$ for the octahedral sheet, $(Si_{3.53}Al_{0.47})^{0.47-}$ for the tetrahedral sheets within the 2:1 layer, and $(Al_{1.08}Fe_{1.08}Mg_{0.84})^{1.08+}$ for the interlayer brucite layer.

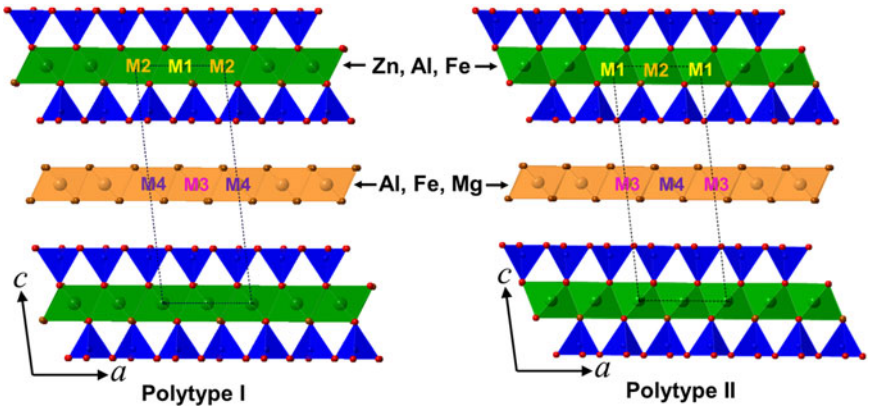


Figure 5. (Color online) Polyhedral models showing crystal structure of baileychlore polytypes (types I and II).

https://doi.org/10.1017/S0885715617000410 Published online by Cambridge University Press

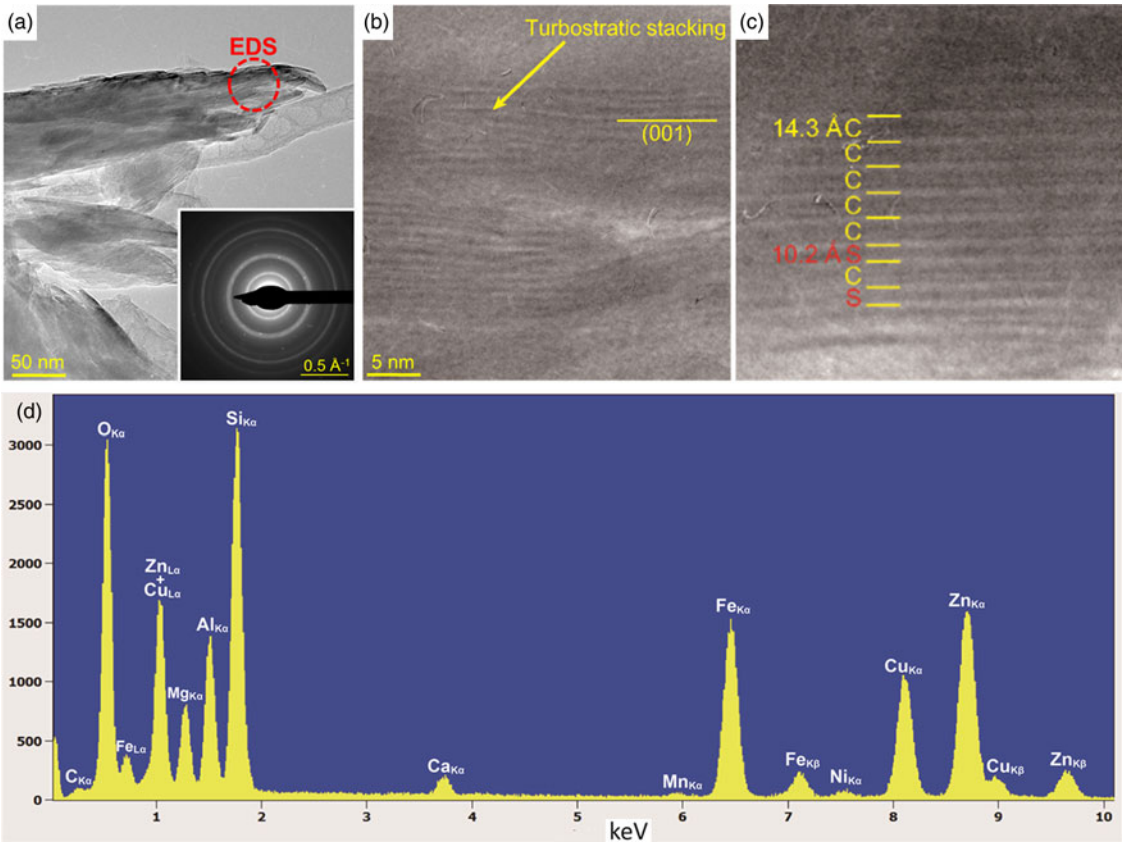


Figure 6. (Color online) (a) Bright-field TEM image of baileychlore showing the continuous SAED rings, indicating the turbostratic disorder in stacking, (b) HRTEM image showing the turbostratic structure, (c) HRTEM image show smectite "S" layers within baileychlore "C", and (d) representative X-ray EDS spectra of baileychlore. Cu peaks are from TEM lacey carbon-coated Cu grid that holds the specimen.

The structural formula suggests the total net negative charge of TOT layers is −1.08. In addition, zinc prefers to enter the octahedral (M1 and M2) sites in the TOT layers (Figure 5). An electron-density projection study also shows that the zinc is stable in the M1 and M2 sites (Rule and Radke, 1988).

Low-magnification bright-field TEM images and SAED of baileychlore show that it is poorly crystalline [Figure 6(a)]. The small crystal size and highly variable orientation are associated with bending of the crystal (Jiang *et al.*, 1990). The high-resolution TEM (HRTEM) images show only basal (001) lattice fringes [Figures 6(b) and 6(c)]. Figure 6(c) shows the smectite interlayers within baileychlore layers. The ~10 Å thickness of smectite was caused by dehydration in the high-vacuum condition (Lee and Peacor, 1985). The TEM–EDS spectra show that baileychlore is associated with Zn, Fe, Mg, Ni, and Mn [Figure 6(d)]. The small amount of Ca detected by EDS is not from calcite as in previous report, but from the interstratified smectite layers.

SUPPLEMENTARY MATERIAL

The supplementary material for this article can be found at https://doi.org/10.1017/S0885715617000410.

ACKNOWLEDGMENTS

This study was supported by the NASA Astrobiology Institute (N07-5489). The authors thank Audrey C. Rule for preserving the samples in Bailey collection. The authors also acknowledge Bruker AXS Inc. for TOPAS 5 program.

Bailey, S. W. (**1988**). "X-ray identification of the polytypes of mica, serpentine, and chlorite," Clays Clay Miner. **36**, 193-213.

Bailey, S. W. and Brown, B. E. (**1962**). "Chlorite polytypism: I. Regular and semi-random one layer structures," Am. Mineral. **47**, 819–850.

Bayliss, P. (**1975**). "Nomenclature of the trioctahedral chlorites," Can. Miner. **13**, 178–180.

Bowman, J. R., Perry, W. T., Kropp, W. P., and Kruer, S. A. (**1987**). "Chemical and isotopic evolution of hydrothermal solutions at Bingham," Utah. Econ. Geol. **82**, 395–428.

Chernosky, J. V. Jr., Berman, R. G., and Bryndzia, L. T. (**1988**). "Stability, phase relations, and thermodynamic properties of chlorite and serpentine group minerals," in *Mineralogical Society of America Reviews in Mineralogy*, edited by S. W. Bailey, Vol. 19, pp. 295-341.

Dunn, P. J., Peacor, D. R., Ramik, R. A., Su, S. C., and Rouse, R. C. (**1987**). "Franklinfurnaceite, a Ca-Fe^{3+}-Mn^{3+}-Mn^{2+} zincosilicate isotropic with chlorite from Franklin, New Jersey," Am. Mineral. **72**, 812–816.

Jacquat, O., Voegelin, A., Villard, A., Marcus, M. A., and Kretzchmar, R. (**2008**). "Formation of Zn-rich phyllosilicate, Zn-layered double hydroxide and hydrozincite in contaminated calcareous soils," Geochim. Cosmochim. Acta **72**, 5037–5054.

Jiang, W. T., Peacor, D. R., Merriman, R. I., and Roberts, B. (**1990**). "Transmission and analytical electron microscopic study of mixed-layer illite-smectite formed as an apparent replacement product of diagenetic illite," Clays Clay Miner. **38**, 449–468.

Laird, J. (**1988**). "Chlorites: metamorphic petrology," in *Mineralogical Society of America Reviews in Mineralogy*, edited by S. W. Bailey, Vol. 19, pp. 405–453.

Lee, J. H. and Peacor, D. R. (**1985**). "Ordered 1:1 interstratification of illite and chlorite: a transmission and analytical electron microscopy study," Clays Clay Miner. **33**, 463–467.

https://doi.org/10.1017/S0885715617000410 Published online by Cambridge University Press

Olives, J. (**1985**) "Biotites and chlorites as interlayered biotite-chlorite crystals," Bull. Mineral. **108**, 635–641.

Reynolds, R. C. (**1988**). "Mixed layer chlorite minerals," in *Mineralogical Society of America Reviews in Mineralogy*, edited by S. W. Bailey, Vol. 19, pp. 601–629.

Rule, A. C. and Radke, R. (**1988**). "Baileychlore, the Zn end member of the trioctahedral chlorite series," Am. Mineral. **73**, 135–139.

Shau, Y. H., Peacor, D. R., and Essene, E. J. (**1990**). "Corrensite and mixed-layer chlorite/corrensite in metabasalt from northern Taiwan: TEM AEM, EMPA, XRD, and optical studies," Contrib. Mineral. Petrol. **105**, 123–142.

Smith, J. T. (**1985**). A mineralized solution collapse breccia, Red Dome, Mungana, North Queensland. B.Sc. thesis, James Cook University, Townsville, North Queensland.

Torrey, C. D., Karjalainen, H., Joyce, P. J., Erceg, M., and Stevens, M. (**1986**). "Geology and mineralization of the Red Dome (Mungana) gold skarn deposit, North Queensland, Australia," in *EGRU Contribution No' 21* (Geology Department, James Cook University, Townsville, North Queensland).

Veblen, D. R. (**1992**). "Electron microscopy applied to nonstoichiometry, polysomatism, and replacement reactions in minerals," in *Mineralogical Society of America Reviews in Mineralogy*, edited by P. R. Buseck, Vol. 27, pp. 181-229.

Veblen, D. R. and Ferry, J. M. (**1983**). "A TEM study of the biotite-chlorite reaction and comparison with petrologic observations," Am. Mineral. **68**, 1160–1168.

Walker, J. R. (**1993**). "Chlorite polytype geothermometry," Clays Clay Miner. **41**, 260–267.

Xu, H. and Veblen, D. R. (**1993**). "Periodic and nonperiodic interstratification in the chlorite-biotite series," Am. Mineral. **81**, 1396–1404.

Xu, H., Luo, G., and Hu, M. (**1990**). "A TEM study of chlorite from Blackhill, Chengde," Chin. J. Mineral. **10**, 204–207.

https://doi.org/10.1017/S0885715617000410 Published online by Cambridge University Press